

Millisecond flash lamp annealing of shallow implanted layers in Ge

C. Wündisch,^{1,a)} M. Posselt,¹ B. Schmidt,¹ V. Heera,¹ T. Schumann,¹ A. Mücklich,¹ R. Grötzschel,¹ W. Skorupa,¹ T. Clarysse,² E. Simoen,² and H. Hortenbach^{3,b)}

¹Forschungszentrum Dresden-Rossendorf, Institute of Ion Beam Physics and Materials Research, P.O. Box 510119, D-01314 Dresden, Germany

²IMEC, Kapeldreef 75, B-3001 Leuven, Belgium

³Qimonda Dresden GmbH & Co OHG, Fraunhofer-Center Nanoelektronische Technologien (CNT), Königsbrücker Strasse 180, D-01099 Dresden, Germany

(Received 3 November 2009; accepted 3 December 2009; published online 23 December 2009)

Shallow n^+ layers in Ge are formed by phosphorus implantation and subsequent millisecond flash lamp annealing. Present investigations are focused on the dependence of P redistribution, diffusion and electrical activation on heat input into the sample and flash duration. In contrast to conventional annealing procedures an activation up to $6.5 \times 10^{19} \text{ cm}^{-3}$ is achieved without any dopant redistribution and noticeable diffusion. Present results suggest that independently of pretreatment the maximum activation should be obtained at a flash energy that corresponds to the onset of P diffusion. The deactivation of P is explained qualitatively by mass action analysis which takes into account the formation of phosphorus-vacancy clusters. © 2009 American Institute of Physics. [doi:10.1063/1.3276770]

Previous investigations on the formation of shallow junctions in Ge by ion beam processing have shown that p^+ doping using boron yields junctions that meet the requirements for the 22 nm technology node, whereas the formation of n^+ junctions by P or As is complicated by the high diffusivity and the low activation of these dopants.¹ The present work deals with millisecond flash lamp annealing (FLA) of shallow layers implanted by P. Dopant redistribution, diffusion, and activation are investigated. The dependence of these effects on flash energy and flash duration is discussed. Furthermore, the influence of pre-amorphization implantation (PAI) and preannealing as well as the solid phase epitaxial recrystallization (SPER) of amorphous layers are studied.

(100) Ge wafers (p -type) with a resistivity between 0.2 and 0.5 $\Omega \text{ cm}$ were used. In order to prevent surface degradation by implantation and outdiffusion during annealing the wafers were capped with 10 nm SiO_2 by sputter deposition. Selected samples were preamorphized by Ge implantation at an energy of 200 keV and a fluence of 10^{15} cm^{-2} . All samples were implanted by P at 30 keV and $3 \times 10^{15} \text{ cm}^{-2}$. The ion beam was tilted by 7° with respect to the normal of the sample surface. Some samples were first preannealed in N_2 ambient at 400 °C for 240 s. Flash-lamp annealing of all samples was carried out in Ar ambient using flash durations of 3 and 20 ms and different electrical energies required to produce the flash. The electrical energy is determined by the capacitors used in the flash lamp facility and the applied voltage. Details of the FLA equipment were elucidated elsewhere.² In a limited range the temperature of the sample is assumed to be proportional to the electrical energy of the flash E_{FLA} and, therefore, can be estimated by

$T = cE_{\text{FLA}} + T_0$. The parameters c and T_0 are determined by complete SPER (Refs. 3 and 4) at about 600 °C and by melting of the sample surface at about 937 °C (3 ms flash: $c = 5.81 \text{ kJ}^{-1} \text{ K}$, $T_0 = 373 \text{ °C}$; 20 ms flash: $c = 2.31 \text{ kJ}^{-1} \text{ K}$, $T_0 = 401 \text{ °C}$). In the following the flash energy E_{FLA} is always used as a measure for the heat transfer to the sample.

Analysis by channeling Rutherford backscattering spectrometry (RBS/C) and cross-sectional transmission electron microscopy (XTEM) showed that the thickness of the amorphous layer formed by the PAI is about 178 nm, whereas the P implantation produces an amorphous layer of about 78 nm thickness. Furthermore, RBS/C and XTEM revealed that preannealing leads to complete SPER of the amorphous layers. If preannealing is not applied, samples recrystallize during FLA. The only exception is that treatment of preamorphized samples by 3 ms flashes leads to the formation of a polycrystalline layer by spontaneous nucleation and recrystallization.^{4,5} In the recrystallized samples end-of-range defects cannot be found by XTEM. This is in contrast to silicon where such defects are always observed after SPER.

Depth profiles of P before and after annealing are shown in Fig. 1. The data were obtained by secondary ion mass spectrometry (SIMS). The difference between the as-implanted profiles in single-crystalline and preamorphized Ge is due to suppressed channelling in the latter case. Preannealing at 400 °C for 240 s leads to fast phosphorus redistribution by the snow plough effect [Figs. 1(a) and 1(b)]. A certain amount of P is incorporated into crystalline Ge, and the surplus is pushed ahead from the moving amorphous-crystalline interface. This leads to P loss of about 25% and the level of incorporation is about $3 \times 10^{20} \text{ cm}^{-3}$. This value can be obtained from the plateau in the profiles shown in Figs. 1(a) and 1(b). The level of P incorporation found during SPER at 400 °C is higher than the maximum equilibrium solubility known from literature ($2 \times 10^{20} \text{ cm}^{-3}$, cf. Refs. 1, 6, and 7) and is therefore called metastable solubility.^{8,9} On the other hand, SPER during FLA [Figs. 1(c) and 1(d)] does not show any significant snow plough effect. Obviously,

^{a)} Author to whom correspondence should be addressed. Forschungszentrum Dresden-Rossendorf, Institute of Ion Beam Physics and Materials Research, P.O. Box 510119, D-01314 Dresden, Germany. Electronic mail: c.wuendis@fzd.de.

^{b)} Present address: SGS Institut Fresenius GmbH, Zur Wetterwarte 10, D-01109 Dresden, Germany.

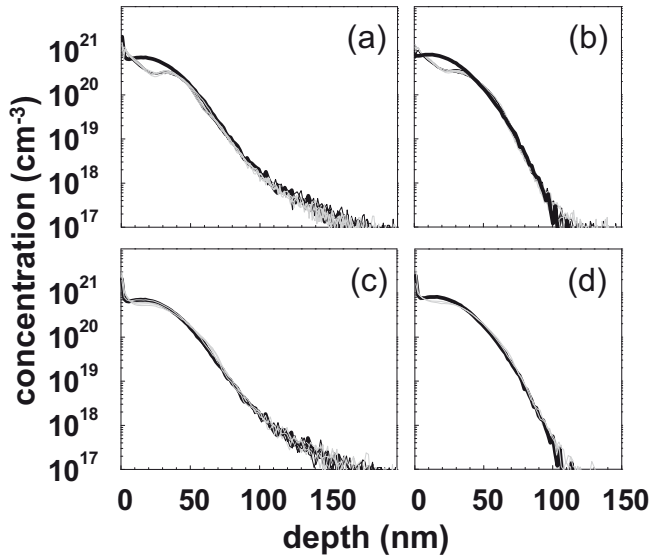


FIG. 1. Depth profiles of P in samples prepared without [(a) and (c)] and with [(b) and (d)] PAI as well as with [(a) and (b)] and without [(c) and (d)] preannealing. The as-implanted profiles are shown by thick black lines. Thin black and gray lines show P depth distributions after flash lamp annealing (FLA) for 3 and 20 ms, respectively. In the cases of 3 and 20 ms flashes the flash energy varied between 39 and 80 kJ as well as between 86 and 139 kJ, respectively.

nearly all phosphorus atoms are incorporated into crystalline Ge. This may be due to the fact that the temperature during SPER at millisecond FLA is higher than during preannealing, leading to a metastable solubility of at least $5-7 \times 10^{20} \text{ cm}^{-3}$. The temperature dependence of the metastable solubility can be explained by the competition between the mobility of the impurity in the amorphous phase and the velocity of SPER (cf. Refs. 9 and 10, and references therein). The higher the temperature, the higher the speed of the amorphous-crystalline interface, the less likely the impurity can stay in front of it and, therefore, incorporation into the crystalline phase prevails.

Figures 1(a)–1(d) clearly demonstrate that no P diffusion occurs if the flash energy does not exceed 80 and 139 kJ for 3 and 20 ms flash duration, respectively. This is in striking contrast to conventional annealing with durations of seconds to hours. Significant concentration-dependent P diffusion is already observed in the case of annealing at 500 °C for 60 s.^{8,11} However, some diffusion is also found at higher flash energies of 88 kJ (3 ms) and 183 kJ (20 ms) as shown in Fig. 2(a). In this case the temperature of the sample is so high that diffusion can even occur during some milliseconds. If the flash energy is further increased the near surface region of the sample melts and a huge diffusion of phosphorus is found [Fig. 2(b)].

The variable probe spacing technique¹² and micro-four-point-probe measurements¹³ were applied to determine the sheet resistance of the samples.¹⁴ Figures 3(a) and 3(c) depict the sheet resistance of the samples annealed by FLA for 3 and 20 ms, respectively. The flash energy E_{FLA} is given on the abscissa. In Fig. 3 data points obtained by the same preparation method are marked by the same symbols. These points are connected by straight lines if no P diffusion is observed [cf. Figs. 1(a)–1(d)] whereas the isolated points indicate diffusion in the solid phase [cf. Fig. 2(a)]. Since it is not useful to compare sheet resistance data for active layers with different depth distributions of charge carriers, the elec-

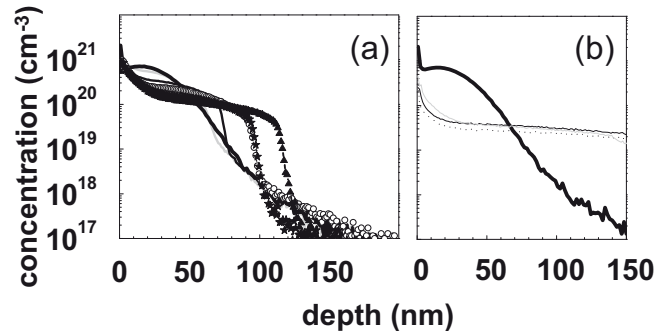


FIG. 2. P depth distributions obtained after different pretreatments and FLA at higher flash energies than in the case of Fig. 1. (a) Thin gray and black lines show the case of 3 ms FLA at 88 and 97 kJ, respectively, for samples without any pretreatment. The curves with lines and symbols were obtained for 20 ms FLA at 182 kJ (open circles – without any pretreatment, triangles-PAI, stars-PAI and preannealing). (b) Thin lines depict results obtained for 20 ms FLA at 232 kJ (black line – without any pretreatment, dotted line – PAI, gray line – PAI and preannealing).

trical properties are discussed in terms of the activation level of dopants. This quantity was roughly estimated using both the SIMS profile obtained after annealing and the corresponding value of sheet resistance.¹⁵ The relation by Cuttriss¹⁶ was used in order to transform resistivity to carrier concentration data. The resulting values for the activation are shown in Figs. 3(b) and 3(d). The figures demonstrate that below a certain threshold the activation level increases with increasing heat transfer to the sample, independently of the pretreatment. This effect is more pronounced for 3 ms flash duration. Below a certain flash energy preannealed samples show a lower activation than those without this treatment. If preannealing is used, samples that underwent PAI show a higher activation. In the case of 20 ms flash duration samples that did not undergo preannealing have a higher activation if they were preamorphized. The similar case for 3 ms duration was not investigated since a polycrystalline layer was formed.

The highest activation level of about $6.5 \times 10^{19} \text{ cm}^{-3}$ is achieved for the 3 ms flash and 97 kJ electrical energy. This corresponds to a case where slight P diffusion is observed

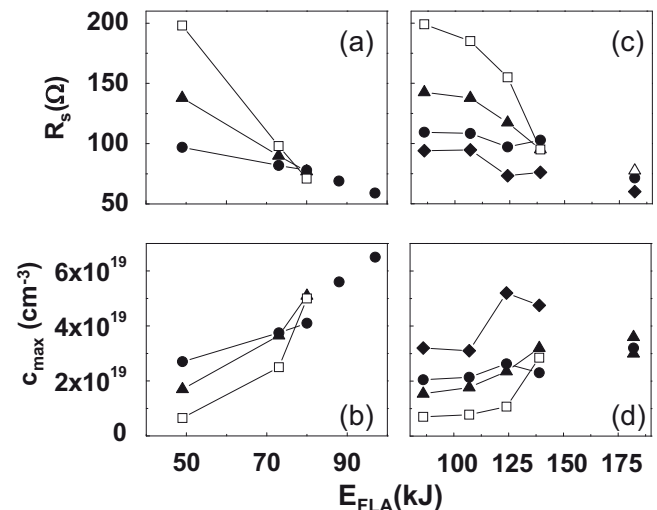


FIG. 3. Sheet resistance R_s and maximum carrier concentration c_{max} in the case of 3 ms [(a) and (b)] and 20 ms [(c) and (d)] FLA, for different flash energies and pretreatments. Circles: without any pretreatment, open squares: preannealing, diamonds: PAI, triangles: PAI and preannealing.

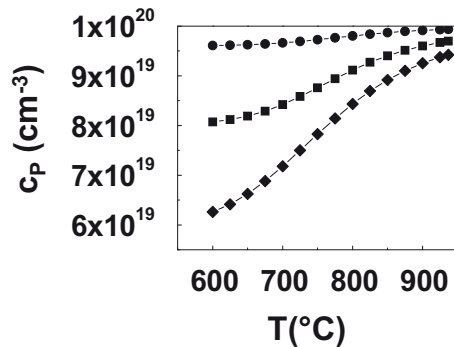


FIG. 4. Result of mass action analysis taking into account the formation of P_nV clusters ($n=1\dots4$): concentration of unbound or active P vs temperature. Different values are assumed for the total vacancy concentration (circles: 10^{18} cm^{-3} squares: 5×10^{18} cm^{-3} , diamonds: 10^{19} cm^{-3}), and the total concentration of P is 10^{20} cm^{-3} .

[cf. Fig. 2(a)]. However, the comparison with results for the 20 ms flash shows that the activation level does not increase significantly or even decreases if P diffusion becomes stronger [cf. Figs. 3(d) and 2(a)]. Therefore, the optimum should be found at that electrical energy of the flash that corresponds to the onset of P diffusion. Taking into account the data depicted in Figs. 3(b) and 3(d) it may be concluded that this optimum should not strongly depend on the pretreatment. However, the highest activation level of P obtained in this work is far below the metastable and the equilibrium solubility. The fact that solubility returns to the equilibrium value during annealing after the completion of SPER or in subsequent annealing steps was also reported for dopants in Si. The reduction of solubility leads to less dopants on substitutional sites and to a concentration of activated dopants below or equal to equilibrium solubility. The decrease of solubility and activation may be accompanied by the formation of dopant-defect clusters.^{9,17-19} However, in the considered samples such clusters were not found by XTEM. Therefore, it is assumed that deactivation is due to the formation of P-vacancy (PV) acceptor pairs¹ or other tiny clusters containing vacancies and dopant atoms²⁰ which are hardly detectable by standard XTEM. Indeed calculations using density functional theory and mass action analysis showed that the formation of P_nV clusters ($n=1, \dots, 4$) may be responsible for the deactivation of P.²¹ Using the data from Ref. 21 a similar mass action analysis was performed. The temperature dependence of the concentration of unbound P is depicted in Fig. 4. In order to demonstrate qualitatively the effect of deactivation a total P concentration (10^{20} cm^{-3}) below equilibrium solid solubility is assumed and different values for the total concentration of vacancies were considered. These values are much higher than the equilibrium vacancy concentration due to defect formation by ion implantation. Fig-

ure 4 can be used to interpret the dependence of the P activation on flash energy and pretreatment: At low temperatures (or flash energies) and/or at high vacancy concentration many P_nV clusters are formed and, therefore, a relatively low level of unbound or electrically active P is found. At higher temperature and/or lower concentration of vacancies the concentration of active P increases. It should be emphasized that present mass action analysis considers equilibrium states as well as a homogeneous distribution of P and vacancies. Kinetics could prevent the ability of the system to reach such states so that the above interpretation should be used with some caution.

- ¹E. Simoen, A. Satta, A. D'Amore, T. Janssens, T. Clarysse, K. Martens, B. De Jaeger, A. Benedetti, I. Hoflijk, B. Brijs, M. Meuris, and W. Vandervorst, *Mater. Sci. Semicond. Process.* **9**, 634 (2006).
- ²W. Skorupa, D. Panknin, W. Anwand, M. Voelskow, G. Ferro, Y. Monteil, A. Leycuras, J. Pezoldt, R. McMahon, M. Smith, J. Camassel, J. Stoenenos, E. Polychroniadis, P. Godignon, N. Mestres, D. Turover, S. Rushworth, and A. Friedberger, *Mater. Sci. Forum* **457**, 175 (2004).
- ³L. Csepregi, R. P. Küllen, J. W. Mayer, and T. W. Sigmon, *Solid State Commun.* **21**, 1019 (1977).
- ⁴B. C. Johnson, P. Gortmaker, and J. C. McCallum, *Phys. Rev. B* **77**, 214109 (2008).
- ⁵G. L. Olson and J. A. Roth, *Mater. Sci. Rep.* **3**, 1 (1988).
- ⁶V. I. Fistul, A. G. Yakovenko, A. A. Gvelesiani, V. N. Tsygankov, and R. L. Korchazhkina, *Inorg. Mater.* **11**, 457 (1975).
- ⁷F. A. Trumbore, *Bell Syst. Tech. J.* **39**, 205 (1960).
- ⁸A. Satta, E. Simoen, R. Duffy, T. Janssens, T. Clarysse, A. Benedetti, M. Meuris, and W. Vandervorst, *Appl. Phys. Lett.* **88**, 162118 (2006).
- ⁹R. Duffy, V. C. Venezia, K. van der Tak, M. J. P. Hopstaken, G. C. J. Maas, F. Roozeboom, Y. Tamminga, and T. Dao, *J. Vac. Sci. Technol. B* **23**, 2021 (2005).
- ¹⁰R. G. Elliman and Z. W. Fang, *J. Appl. Phys.* **73**, 3313 (1993).
- ¹¹M. Posselt, B. Schmidt, W. Anwand, R. Grötzschel, V. Heera, A. Mücklich, C. Wündisch, W. Skorupa, H. Hortenbach, S. Gennaro, M. Bersani, D. Giubertoni, A. Möller, and H. Bracht, *J. Vac. Sci. Technol. B* **26**, 430 (2008).
- ¹²T. Clarysse, D. Vanhaeren, I. Hoflijk, and W. Vandervorst, *Mater. Sci. Eng. R* **47**, 123 (2004).
- ¹³T. Clarysse, W. Vandervorst, R. Lin, D. H. Petersen, and P. F. Nielsen, *Nucl. Instrum. Methods Phys. Res. B* **253**, 136 (2006).
- ¹⁴G. Hellings, C. Wündisch, G. Eneman, E. Simoen, T. Clarysse, M. Meuris, W. Vandervorst, M. Posselt, and K. De Meyer, *Electrochem. Solid-State Lett.* **12**, H417 (2009).
- ¹⁵W. Lerch, S. Paul, J. Niess, F. Cristiano, Y. Lamrani, P. Calvo, N. Cherkashin, D. F. Downey, and E. A. Arevalo, *J. Electrochem. Soc.* **152**, G787 (2005).
- ¹⁶D. B. Cuttris, *Bell Syst. Tech. J.* **40**, 509 (1961).
- ¹⁷Y. Takamura, S. H. Jain, P. B. Griffin, and J. D. Plummer, *J. Appl. Phys.* **92**, 230 (2002).
- ¹⁸Y. Takamura, P. B. Griffin, and J. D. Plummer, *J. Appl. Phys.* **92**, 235 (2002).
- ¹⁹Y. Takamura, A. Vailionis, A. F. Marshall, P. B. Griffin, and J. D. Plummer, *J. Appl. Phys.* **92**, 5503 (2002).
- ²⁰W. Anwand, W. Skorupa, Th. Schumann, M. Posselt, B. Schmidt, R. Grötzschel, and G. Brauer, *Appl. Surf. Sci.* **255**, 81 (2008).
- ²¹A. Chroneos, H. Bracht, R. W. Grimes, and B. P. Uberuaga, *Mater. Sci. Eng., B* **154**, 72 (2008).